1980-09

# Investigation of the use of liquid crystal thermography study flow over turbomachinery blades

Brennon, Roy L.

Naval 106

# NAVAL POSTGRADUATE SCHOOL
## Monterey, California


# THESIS

INVESTIGATION OF THE USE
OF LIQUID CRYSTAL THERMOGRAPHY
TO STUDY FLOW OVER TURBOMACHINERY BLADES

by

Roy L. Brennon

September 1980

Thesis Advisor: Matthew D. Kelleher

Approved for public release; distribution unlimited

## REPORT DOCUMENTATION PAGE

READ INSTRUCTIONS BEFORE COMPLETING FORM

| | |
|---|---|
| 1. REPORT NUMBER | 2. GOVT ACCESSION NO. / 3. RECIPIENT'S CATALOG NUMBER |
| 4. TITLE (and Subtitle): Investigation of the Use of Liquid Crystal Thermography to Study Flow Over Turbomachinery Blades | 5. TYPE OF REPORT & PERIOD COVERED: Master's Thesis; September 1980 |
| | 6. PERFORMING ORG. REPORT NUMBER |
| 7. AUTHOR(s): Roy L. Brennon | 8. CONTRACT OR GRANT NUMBER(s) |
| 9. PERFORMING ORGANIZATION NAME AND ADDRESS: Naval Postgraduate School, Monterey, California 93940 | 10. PROGRAM ELEMENT, PROJECT, TASK AREA & WORK UNIT NUMBERS |
| 11. CONTROLLING OFFICE NAME AND ADDRESS: Naval Postgraduate School, Monterey, California 93940 | 12. REPORT DATE: September 1980 |
| | 13. NUMBER OF PAGES: 67 pages |
| 14. MONITORING AGENCY NAME & ADDRESS(if different from Controlling Office): Naval Postgraduate School, Monterey, California 93940 | 15. SECURITY CLASS. (of this report): Unclassified |
| | 15a. DECLASSIFICATION/DOWNGRADING SCHEDULE |

16. DISTRIBUTION STATEMENT (of this Report)
Approved for public release; distribution unlimited

17. DISTRIBUTION STATEMENT (of the abstract entered in Block 20, if different from Report)

18. SUPPLEMENTARY NOTES

19. KEY WORDS (Continue on reverse side if necessary and identify by block number)
liquid crystals, thermography, isotherms, stall angle, separation, laminar separation bubble, convection heat transfer coefficient, boundary layer, angle of incidence, NACA series 65 compressor blade.

20. ABSTRACT (Continue on reverse side if necessary and identify by block number)

The use of liquid crystal thermography was investigated as a technique for visualizing the flow over a NACA series 65 compressor blade. The demonstration of the feasibility of the technique was conducted in the low turbulence wind tunnel at the U.S. Naval Postgraduate School.

Local heat transfer coefficients were obtained for Reynolds numbers varying from 100,000 to 600,000 with the angle of

incidence of the blade varying from 0 degrees to 30 degrees.

Approved for public release; distribution unlimited

# Investigation of the Use of Liquid Crystal Thermography Study Flow Over Turbomachinery Blades

by

Roy L. Brennon
Lieutenant Commander, United States Navy
B.S., United States Naval Academy, 1968

Submitted in partial fulfillment of the
requirement for the degree of

MASTER OF SCIENCE IN MECHANICAL ENGINEERING

from the

NAVAL POSTGRADUATE SCHOOL
September 1980

ABSTRACT

The use of liquid crystal thermography was investigated as a technique for visualizing the flow over a NACA series 65 compressor blade. The demonstration of the feasibility of the technique was conducted in the low turbulence wind tunnel at the U.S. Naval Postgraduate School.

Local heat transfer coefficients were obtained for Reynolds numbers varying from 100,000 to 600,000 with the angle of incidence of the blade varying from 0 degrees to 30 degrees.

TABLE OF CONTENTS

LIST OF FIGURES

## LIST OF SYMBOLS AND ABBREVIATIONS

| | | |
|---|---|---|
| $A$ | - | Area |
| $c$ | - | Chord Length |
| $C_p$ | - | Specific Heat at Constant Pressure |
| $h_c$ | - | Convection Heat Transfer Coefficient |
| $h_r$ | - | Radiation Heat Transfer Coefficient |
| $\bar{h}$ | - | Average Convection Heat Transfer Coefficient |
| $i$ | - | Angle of Incidence |
| $I$ | - | Current |
| $k$ | - | Thermal Conductivity |
| $L$ | - | Length |
| LBL | - | Laminar Boundary Layer |
| LS | - | Laminar Separation |
| $P$ | - | Electric Power |
| $P_{atm}$ | - | Atmospheric Pressure |
| $Q$ | - | Rate of Heat Transfer |
| $R$ | - | Resistance |
| RA | - | Reattachment |
| $T$ | - | Temperature |
| TBL | - | Turbulent Boundary Layer |
| TS | - | Turbulent Separation |
| TW | - | Turbulent Wake |
| $t$ | - | Thickness |

$u$ - Air Velocity

$V$ - Voltage

$x$ - Distance from Leading Edge Along Surface

$y$ - Distance from Centerline

$\delta$ - Boundary Layer Thickness

$\mu$ - Dynamic Viscosity

$\nu$ - Kinematic Viscosity

$\rho$ - Density

Dimensionless Groups

$\overline{Nu}$ - Average Nusselt Number

$Pr$ - Prandtl Number

$Re_c$ - Reynolds Number Based on Chord Length

Subscripts

atm - Atmospheric

b - Blade

c - Based on Chord Length

f - Film

L - Based on Length

x - Based on Distance

$\infty$ - Free Stream Condition

min - Minimum

max - Maximum

o - Initial Condition

ACKNOWLEDGMENT

I would like to thank Professor Kelleher for his interest and guidance during this investigation. The helpful advice on problem modeling provided by Professor Yavanovich from the University of Waterloo, Canada, was also greatly appreciated.

# I. INTRODUCTION

The two essential turbomachinery parts of the gas turbine are the compressor and the turbine. A large part of the work produced by the turbine unit goes into driving of the compressor. The efficiency of the gas turbine engine will decrease dramatically with an increase in the aerodynamic losses in the compressor.

Aerodynamic losses are irreversibilities in the flow caused by profile friction losses, flow separation losses, stall losses, and other secondary losses. Therefore, it is absoluately necessary to have a clear and thorough understanding of the aerodynamic phenomena occurring in the compressor blade system.

The understanding of the flow field through the compressor allows the blade designer to better compute the forces acting on the blades, the location of potential aerodynamic problem areas, and determine favorable blade shapes with lower losses. Chapters 16 and 17 of Ref. 1, contain a complete discussion on the necessity of the designer to understand the flow field over a blade, as part of the design of turbine and compressor units.

The purpose of this investigation was to demonstrate the feasibility of using liquid crystal thermography to visualize the surface characteristics of the flow over

a NACA series 65 compressor blade placed in a forced convection environment.

Cholesteric liquid crystals, when applied to a black surface, exhibit brilliant changes in color over discrete, reproducible temperature bands. Used as a temperature sensor, this allows one to visually observe selected isotherms on the surface. These isotherms can be used to infer the location of points of flow separation and boundary layer reattachment. The area of flow transition and angle of stall could also be determined.

As documented in Ref. 2, earlier experiments using liquid crystals in wind tunnels to study heat transfer rates showed promise but were limited in many ways. The pure liquid crystals deteriorated rapidly with age and the accuracy was strongly influenced by mechanical shear, viewing angle, ultraviolet light, and chemical contamination. An encapsulating process developed by the National Cash Register Company (NCR) using a gelatin in a polyvinyl alcohol binder coating greatly reduced or eliminated these problems. These crystals, referred to as encapsulated liquid crystals, are small spheroids with diameters on the order of 20-50 microns.

Previous work at the Naval Postgraduate School using encapsulated liquid crystals included an investigation of the temperature field produced by a cryosurgical probe embedded in a clear gelatin-water test medium [Ref. 3].

Experiments using heated cylinders, in a crossflow of air, covered with the encapsulated liquid crystals were mapped by Meyer in Ref. 2 and Field in Ref. 5. A thesis by Durao [Ref. 6], investigated heat transfer in straight and curved rectangular ducts using liquid crystal thermography.

In the present investigation, data were obtained on a NACA series 65 compressor blade covered with carbon impregnated paper that had a uniform electrical resistivity. The surface of the blade was electrically heated by passing a known voltage through the paper.

The results obtained in this investigation compared favorably with those in Ref. 7. The ability to determine if the boundary layer was turbulent or laminar became more difficult as the Reynolds number was increased and as the angle of incidence was increased.

## II. DESCRIPTION OF APPARATUS

### A. LIQUID CRYSTALS

Cholesteric liquid crystals are encapsulated in a polyvinyl alcohol binder which extends their useful life to several years. When applied to a black surface, the color of the liquid crystals will shift from red through the entire color spectrum to violet as the temperature is raised. The black surface ensures that all light passing through the liquid crystal film is absorbed, allowing the selectively scattered colors from the cholesteric liquid crystals to be observed. The process is reversible, repeatable, and can be accurately calibrated as to temperature within 0.1 degrees Celsius.

Since each crystal has its own sensitivity and is colorless above and below its operating range, by selecting the proper formulation of crystals a large number of isotherms can be viewed on a given surface at one time.

An example would be the crystal S-40 (40 being the temperature in degrees Celsius at which the onset of red appears). As the temperature is raised to 40.0°C, the colorless crystals start to show red. The color will shift to green at 40.7°C, then to blue at 41.3°C, and finally to violet prior to becoming colorless.

Chloresteric liquid crystals are commercially available beginning at essentially any temperature from -20°C to 250°C. Reference 2 contains a very thorough background on the development of liquid crystals in its applications to the study of convective heat transfer.

## B. TEST BLADE

The test blade profile used in this investigation is the NACA 65 $A_{10}$ series blade with a span of ten inches and a chord of eight inches. It was originally constructed with an epoxy core covered by a thin metal casing. The blade is a typical airfoil shape used in compressors and was procured as original equipment for the Rectilinear Cascade at the U.S. Naval Postgraduate School Turbopropulsion Laboratory. The exact translation of the blade numbering system along with the two profile fairing and camber distribution equations can be found in Ref. 8.

## C. LOW TURBULENCE SUBSONIC WIND TUNNEL

The low turbulence subsonic wind tunnel is of an open circuit design with its intake inside the building and its exhaust outside. The test section is 20 inches by 28 inches at the center and is 8 feet long. The prime mover is a six blade axial fan, located at the downstream end, driven by a variable speed 75 horsepower electric motor. The wind speed is continuously variable from 30 to 300 feet

per second when the test section is clear. When the blade and mounting apparatus is installed, the wind speed ranged from 10 to 290 feet per second. The freestream turbulence intensity is controlled by means of a six inch thick honeycomb flow straightener located at the plenum entrance, followed by up to five interchangeable graded screens and an area contraction of ten to one.

Results of a complete survey of the test section are contained in Ref. 9, and indicated a turbulence intensity range from 0.05% to 0.20%.

## III. EXPERIMENTAL PROCEDURE

### A. TEST BLADE PREPARATION

Previous attempts to use this NACA 65 series airfoil for liquid crystal thermography were unsuccessful due to a short circuit between the blade and the covering material [Ref. 10]. This short circuit could not be eliminated with several coats of TV corona dope and red glyptol. To insure against such a problem during this investigation, the metal plating was completely removed. This plating measured 0.003 inches thick.

To better monitor the surface temperature, eight copper constantan thermocouples were imbedded in the blade along with the two previously installed copper constantan thermocouples. The locations of the ten thermocouples are shown in Figure 1. The epoxy core was then covered with three coats of red glyptol. Prior to attaching to the blade, the temperature monitoring system consisting of the eight additional thermocouples, output meter, and connecting wires were calibrated using the Rosemount Engineering Company Model 913A calibration bath with distilled water and the Model 920A commutating bridge. The output meter used in this investigation is an Omega 2176A Digital Thermometer which reads in two-tenths of a degree Fahrenheit.

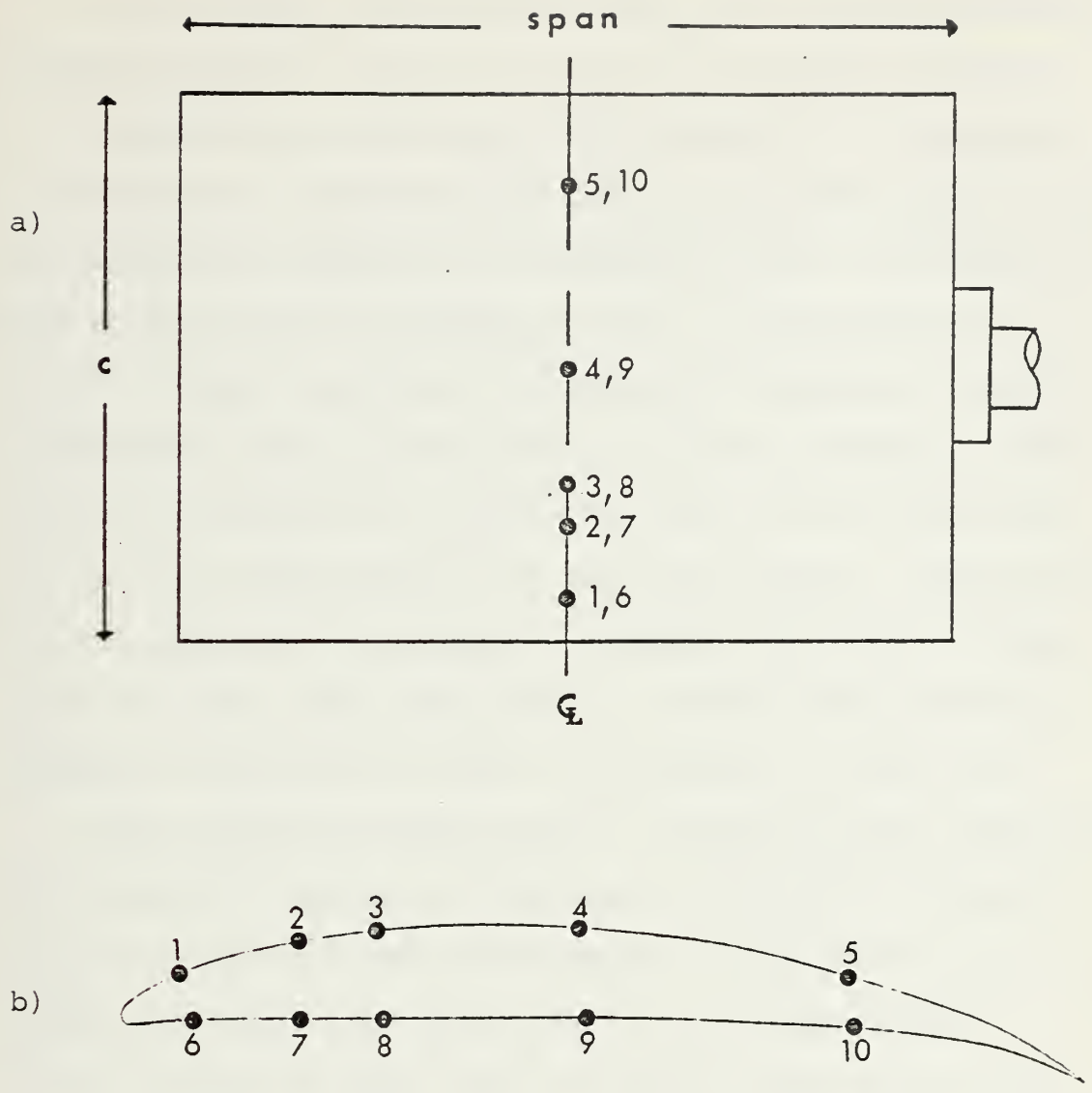


Figure 1. NACA 65 test blade showing location of thermocouples, a) top view, b) side view.

The previous investigation [Ref. 10] has unsuccessfully attempted to use aluminized milar or Teledeltos paper as an electrically conducting cover material for the blade. A commercially produced electrically resistive paper known as Armstrong Temsheet was selected for this investigation due to its success reported in Ref. 5. Temsheet is a thin, highly flexible, electrically resistive, carbon impregnated paper, containing no wires or ribbons. The nominal thickness is 0.038 inches with an electrical resistance of approximately 45 ohms per square. The electrical resistivity is uniform, to within two percent, from point to point over large areas. Scotch Brand Sprament Adhesive was used to attach the temsheet to the blade.

Self-adhering copper strips, attached to the edges of the temsheet, served as connecting points for the power supply. Power to heat the temsheet was provided by a Lambda model LK 345A FM regulated D.C. power supply. A Data Precision Model 1450 voltmeter, connected to the power supply, provided a digital readout of volts used to heat the temsheet. The resistance of the system was measured and found to be 11.7 ohms with no voltage and 11.5 ohms with 40 volts.

A mixture of encapsulated cholesteric liquid crystals, which consisted of R-33, S-40, R-45, and distilled water, was sprayed onto the center seven inches of the test blade

using an X-Acto magic touch air brush with 30 pounds per square inch air pressure. The distilled water was added in the amount necessary to allow the mixture to flow freely through the air brush. After spraying a single coating, the blade was subjected to a portable electric hot air blower to assist the drying of the temsheet and to check the color pattern of the crystals. With ten coats, the colors of the various crystals were adequate to provide the required temperature information.

An investigation by Field in Ref. 5 noted that the liquid crystals fill-in irregularities in the surface of the temsheet leaving a roughness projection size of approximaterly 0.00005 feet.

The calibration results for the liquid crystals used are listed in Appendix B. Figure 2 shows the blade after the temsheet and copper strips were installed.

## B. BLADE INSTALLATION

The NACA 65 series blade was attached to 8.5 inch diameter disks constructed from 0.5 inch thick plexiglass. A blade profile 0.25 inches deep was cut in each disk. The disks were then fitted to the blade and any gaps were filled in with a liquid epoxy to insure a vibration-free slip fit. The disks were fitted into the center of 20 inch by 29 inch plexiglass side panels, 0.5 inches thick, with a half lap joint to give a flush fit when they were mated.

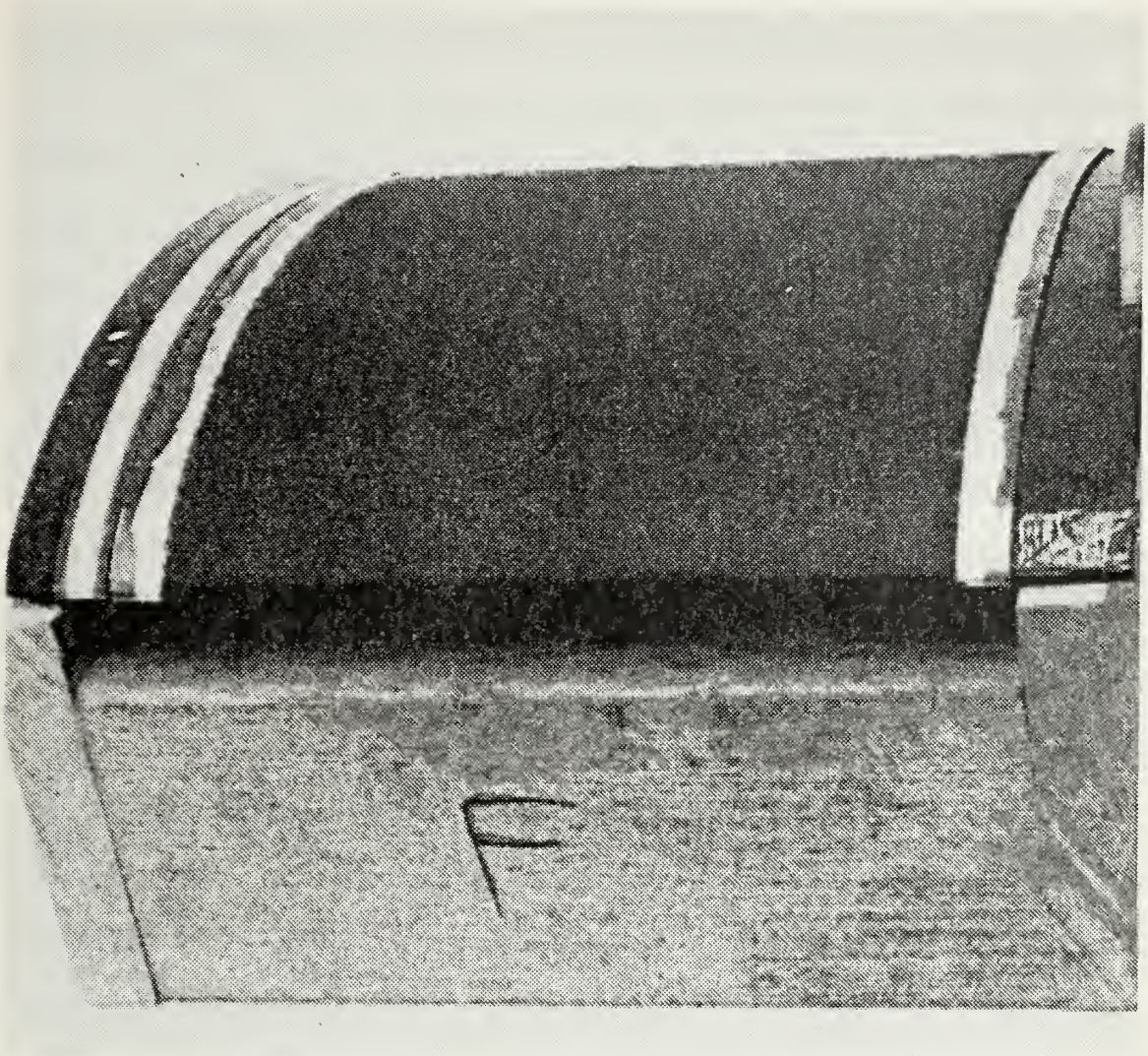

Figure 2. NACA 65 series test blade after temsheet and copper strip installation.

The blade was fitted with a handle so that rotating the blade and disks could be accomplished from outside of the wind tunnel. Rotating the blade could thus be accomplished without having to alter the wind speed controls to increase the angle of incidence. The disks were marked in 5 degree increments on the forward facing 180 degree arc, thereby allowing the angle of incidence to be easily observed through the clear side of the tunnel test section. The side panels were marked as to horizontal and vertical position. A plexiglass window was installed in the bottom of the test section, allowing viewing of the blade from underneath the tunnel. The test blade and side panels were rigidly mounted in the low turbulence wind tunnel above the viewing windown. The location of the isotherms on the blade were recorded with the aid of distance markings placed on each side of the temsheet and straight lines fixed to the viewing window.

Figure 3 shows the final blade setup in the plexiglass support frame. Figure 4 shows the support frame, test blade, and electrical hookup inside the wind tunnel.

## C. BLADE SURFACE TEMPERATURE

The surface temperature on the test blade was determined by the color of the liquid crystals. The thermocouples acted as an aid to determine which crystal was actually being viewed. Appendix B gives the temperatures corresponding to

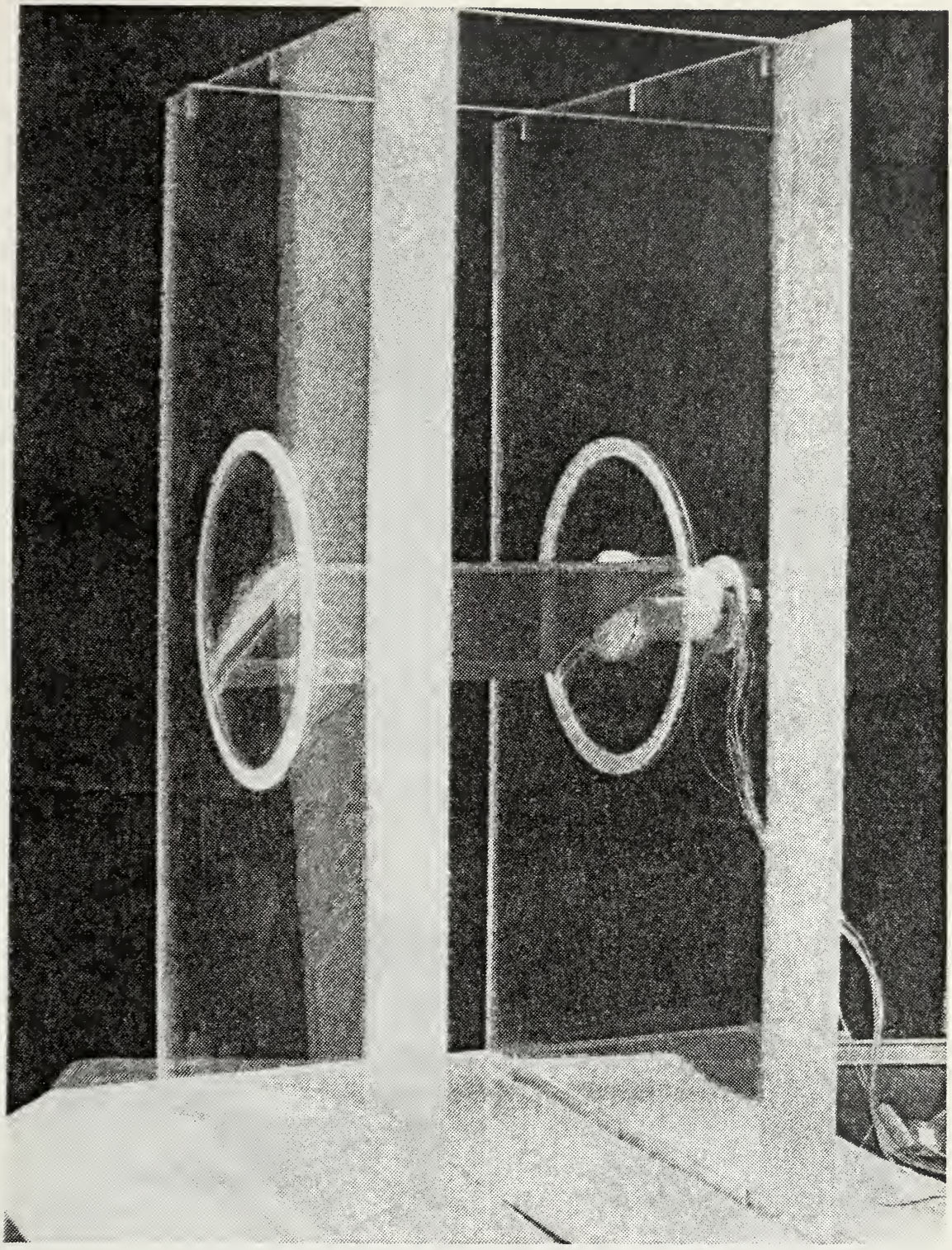

Figure 3. Test blade and support frame prior to installation in the low turbulence subsonic wind tunnel.

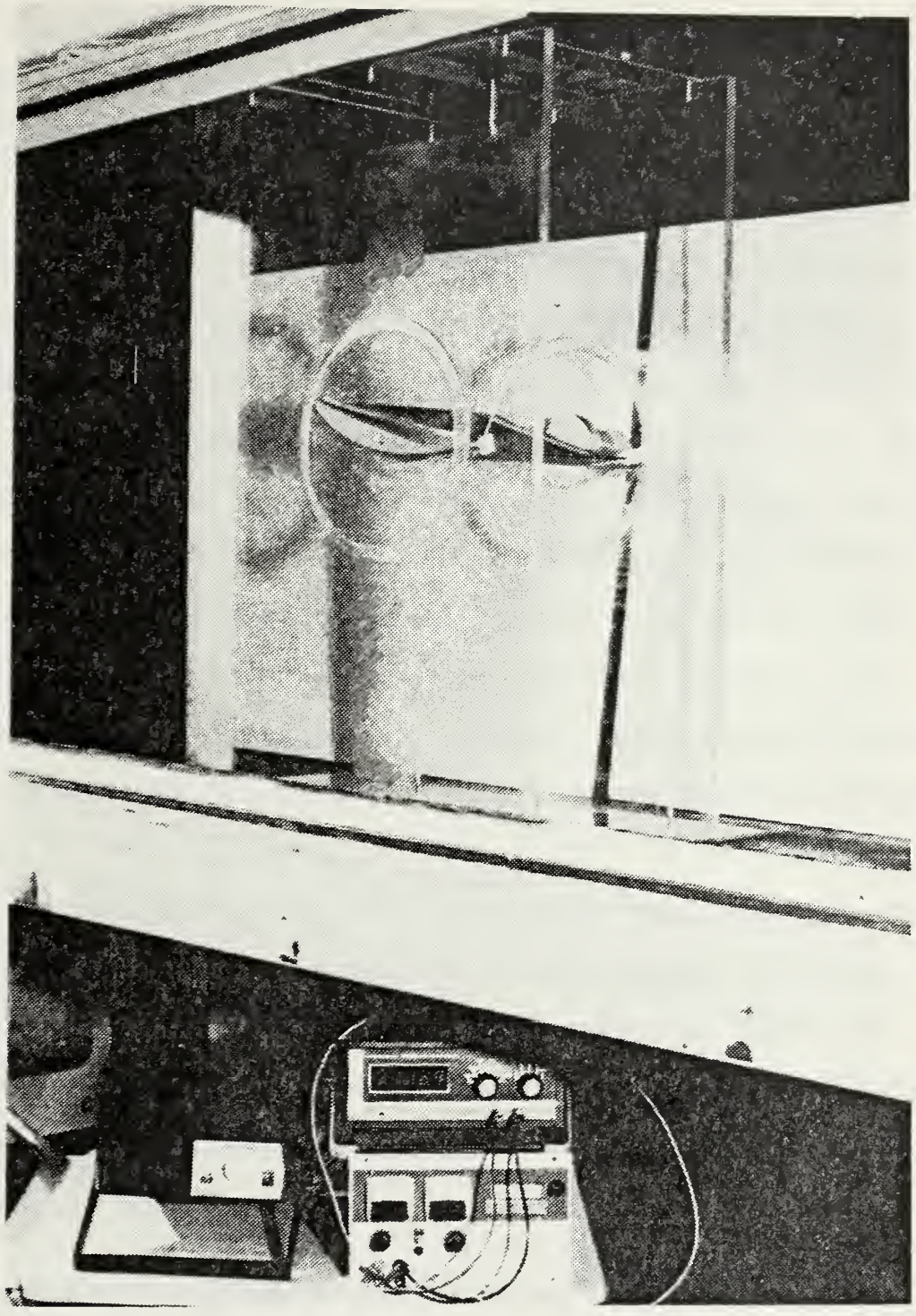

Figure 4. Support frame with the test blade and electrical hook-up inside the low turbulence subsonic wind tunnel.

the crystal/color combination. The location of the start of a certain color band was recorded as the line of the isotherm with the width of the color band giving an indication of the temperature gradient along the blade.

An increase or decrease of the applied voltage with the Reynolds number and angle of incidence held constant, raised or lowered, respectively, the overall surface temperature of the blade. This moved the color bands over the blade, making it possible to obtain a continuous temperature profile of the entire blade by recording the location of the isotherm and crystal/color combination of these isotherms. Scales were attached to each side of the blade, marked in 0.05 inch increments. Sighting lines on the viewing window enabled the isotherm to be recorded within a tolerance of 0.1 inch distance from the blade's leading edge.

To insure a steady state condition when recording the blade surface temperatures, the thermocouples imbedded in the blade under the temsheet were monitored. Once the thermocouple nearest the desired isotherm did not fluctuate more than two-tenths of a degree in a three-minute period, the blade was considered to be in a steady state temperature condition.

D. ANGLE OF INCIDENCE

The actual tilt of the blade with respect to the free stream air direction was recorded as the angle of incidence.

This angle is defined, for this investigation, as the angle between the free stream air direction and a base line drawn between the lowest points on the leading and trailing edges of the blade. These baseline points were established by placing the test blade on a flat surface with the suction surface of the blade up, and marking the pressure surface of the blade at the points of contact between itself and the flat surface. Figure 5 shows a 15° angle of incidence.

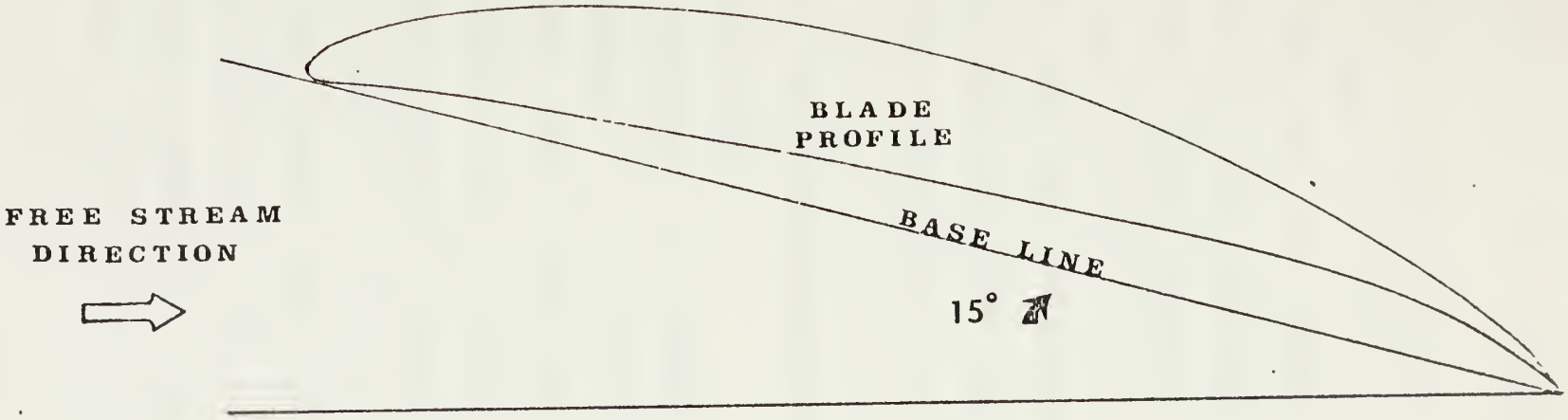


Figure 5. NACA 65 series blade profile showing an angle of incidence of 15 degrees.

## IV. RESULTS

The flow of a real fluid can be analyzed by the changes occurring within the boundary layer that is formed near the surface. Initially, the boundary layer developed is laminar. In laminar flow, fluid particles move along smooth paths with one layer gliding smoothly over an adjacent layer. At some critical distance from the leading edge, depending on the flow field and fluid properties, small disturbances in the flow begin to become amplified, and a transition process takes place until the flow becomes turbulent. The turbulent flow is characterized by a random churning action with chunks of fluid moving in irregular patterns within the boundary layer.

The convection heat transfer coefficients and temperature distributions are functions of both the thickness of the boundary layer and the type of flow within this boundary layer. As the boundary layer increases in thickness with distance from the leading edge and angle of incidence, the fluid velocity is retarded, resulting in an increased thermal resistance to heat transfer. This increased thermal resistance shows up in a decreased value of the convection heat transfer coefficient. The value of the convection heat transfer coefficient would then be smallest at a point

where the kinetic energy of the fluid is attenuated sufficiently so that the fluid in the boundary layer cannot overcomes the adverse pressure gradient present on the surface. At this point the boundary layer separates from the surface.

Flow as classified by Roshko in Ref. 11, can be subcritical, supercritical, or transcritical. Subcritical flow contains only laminar separation. The supercritical flow is characterized by a laminar separation bubble, re-attachment, followed by turbulent separation. With the disappearance of a separation bubble, the flow is in the transcritical range and the separation is not purely turbulent.

Figure 6 depicts a typical subcritical flow pattern and the resulting trends in the convection heat transfer coefficient for flow over a compressor blade. Figure 7 depicts the supercritical flow pattern, with its resulting trends in the convection heat transfer coefficient for flow over a compressor blade.

First, an example of a laminar boundary layer and separation is seen in Figure 8. The value of the local convection heat transfer coefficient continuously decreases from the leading edge to approximately 68% of the distance from the leading edge point. At this point the value of the coefficient increases at a relatively steeper slope. Knowing the angle of incidence (5 degrees), and the Reynolds

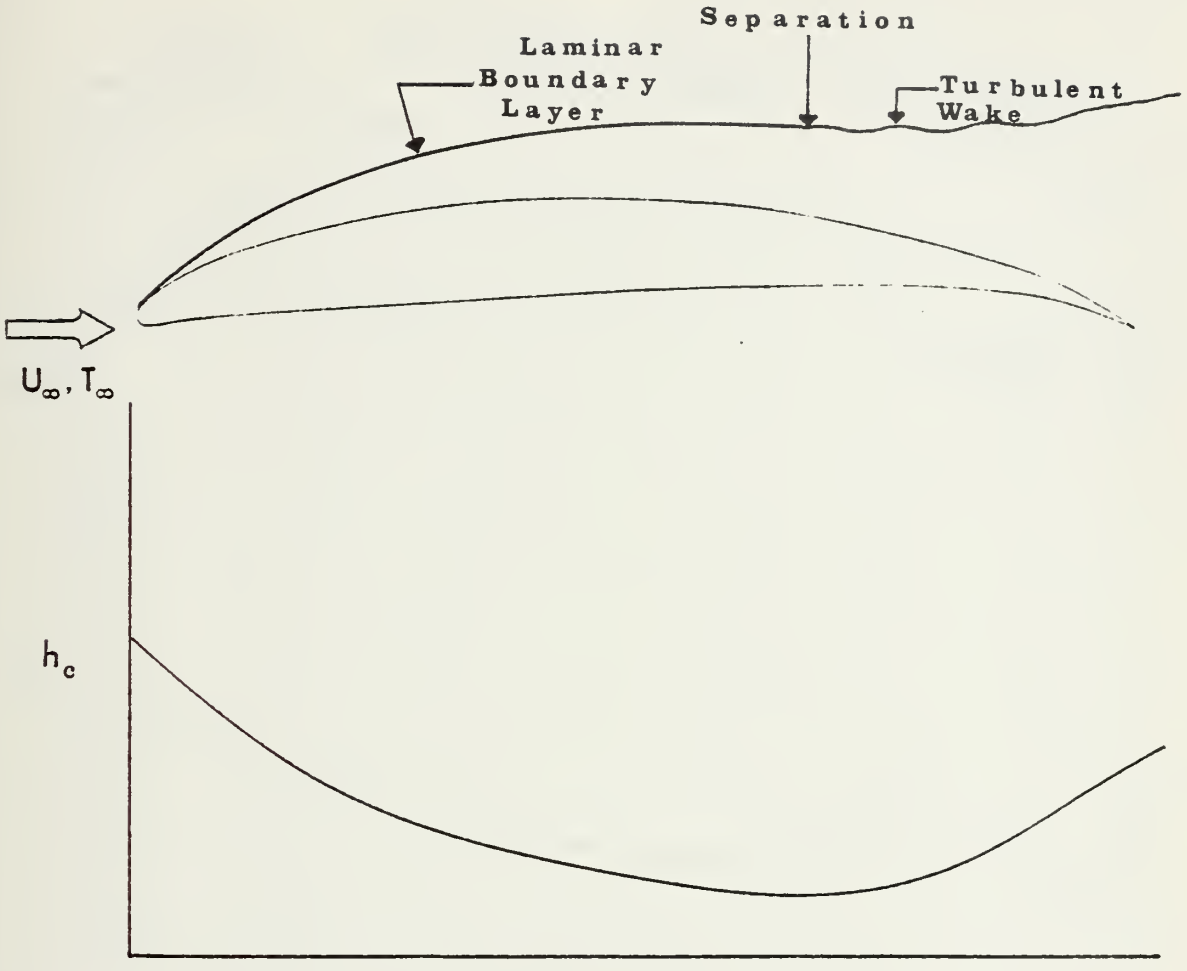


Figure 6. Schematic of a compressor blade in subcritical flow with the resulting convection heat transfer coefficient distribution.

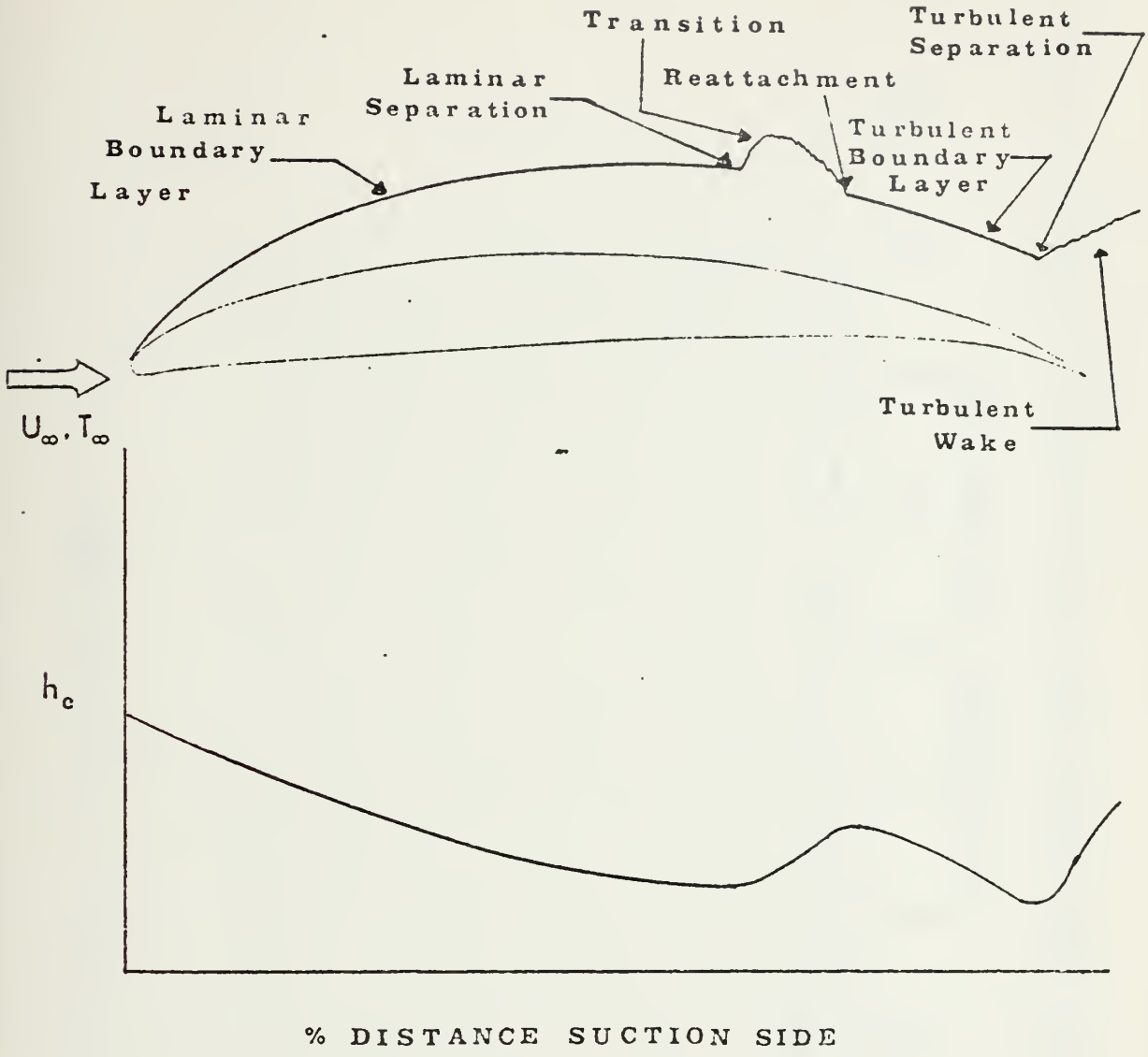


Figure 7. Schematic of a compressor blade in supercritical flow with the resulting convection heat transfer coefficient distribution.

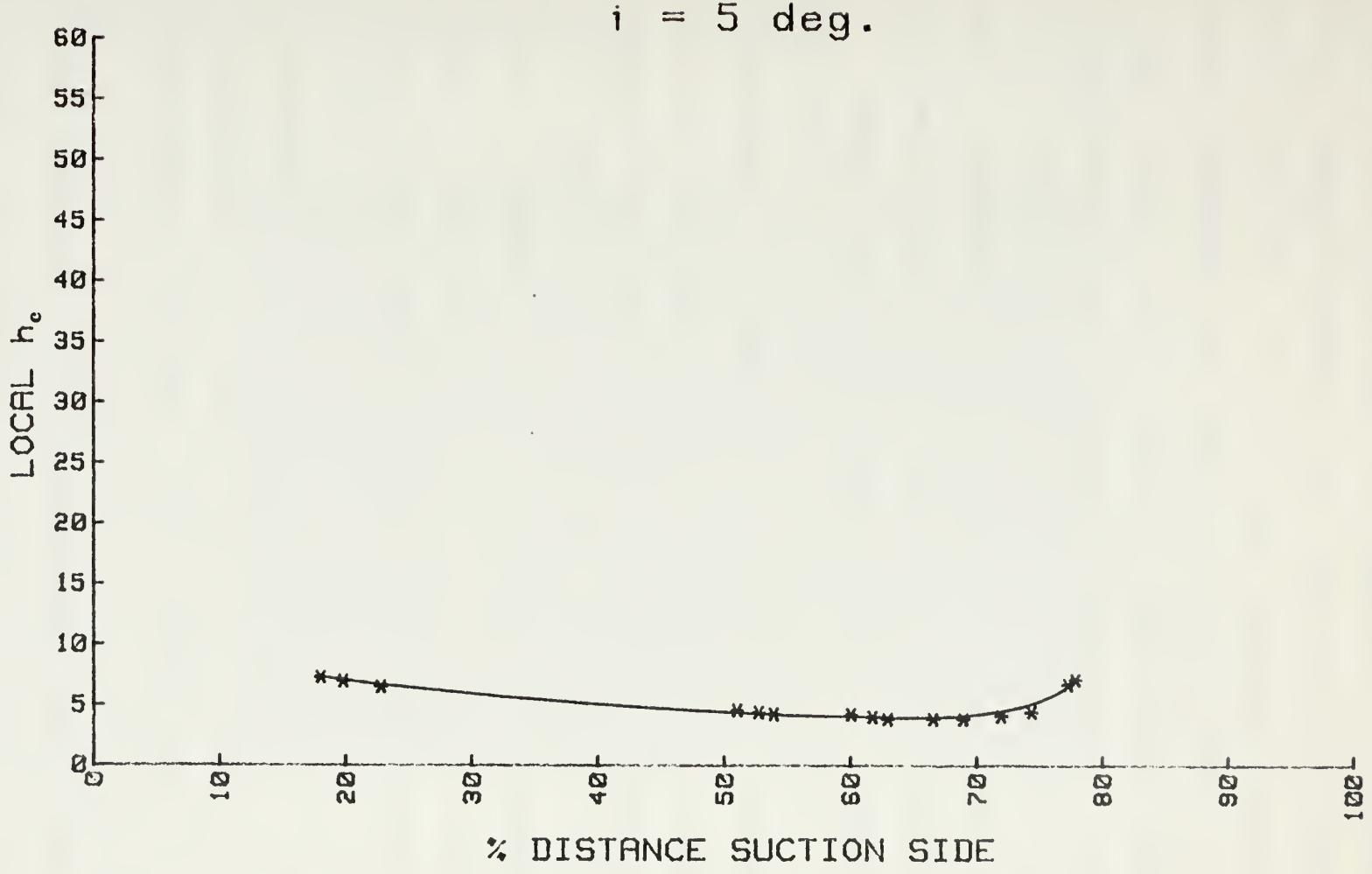


Figure 8. Local convection heat transfer coefficient vs. % of distance from leading edge on suction side of test blade. $Re_c$ = 104,000.

number (104,000 for this configuration), it is inferred that a laminar boundary layer exists until the 68% distance point is reached. The flow then separates from the blade with a turbulent wake remaining over the last 32% of the blade. Figure 9 is a color photograph showing the isotherms using the previously discussed liquid crystals. Starting at the leading edge, the crystals seen are R-33, S-40, and R-45, respectively, until the 68% distance point, then the reverse sequence is seen with much narrower color bands.

Holding the Reynolds number essentially constant and increasing the angle of incidence to 10 degrees, a separation bubble, as discussed in Ref. 11, can be produced. With the test blade in this configuration, the bubble begins at the point of laminar separation, which now has moved closer to the leading edge. From Figure 10, this point of laminar separation and start of the separation bubble is located at the 35% distance point. Over the region of the bubble, the value of the heat transfer coefficient increases due to the cooling effect of the recirculating air inside the bubble [Ref. 12]. At the 70% distance point, the value of the heat transfer coefficient again starts to decrease. This indicates that the flow has now reattached to the blade and a turbulent boundary layer is present. At the 95% distance point, this boundary layer separates to form a turbulent wake as indicated by an upswing in the curve. Figure 11 shows the

Figure 9. NACA test blade, i = 5 degrees, $Re_c$ = 104,000. Suction side, air flow from top to bottom.

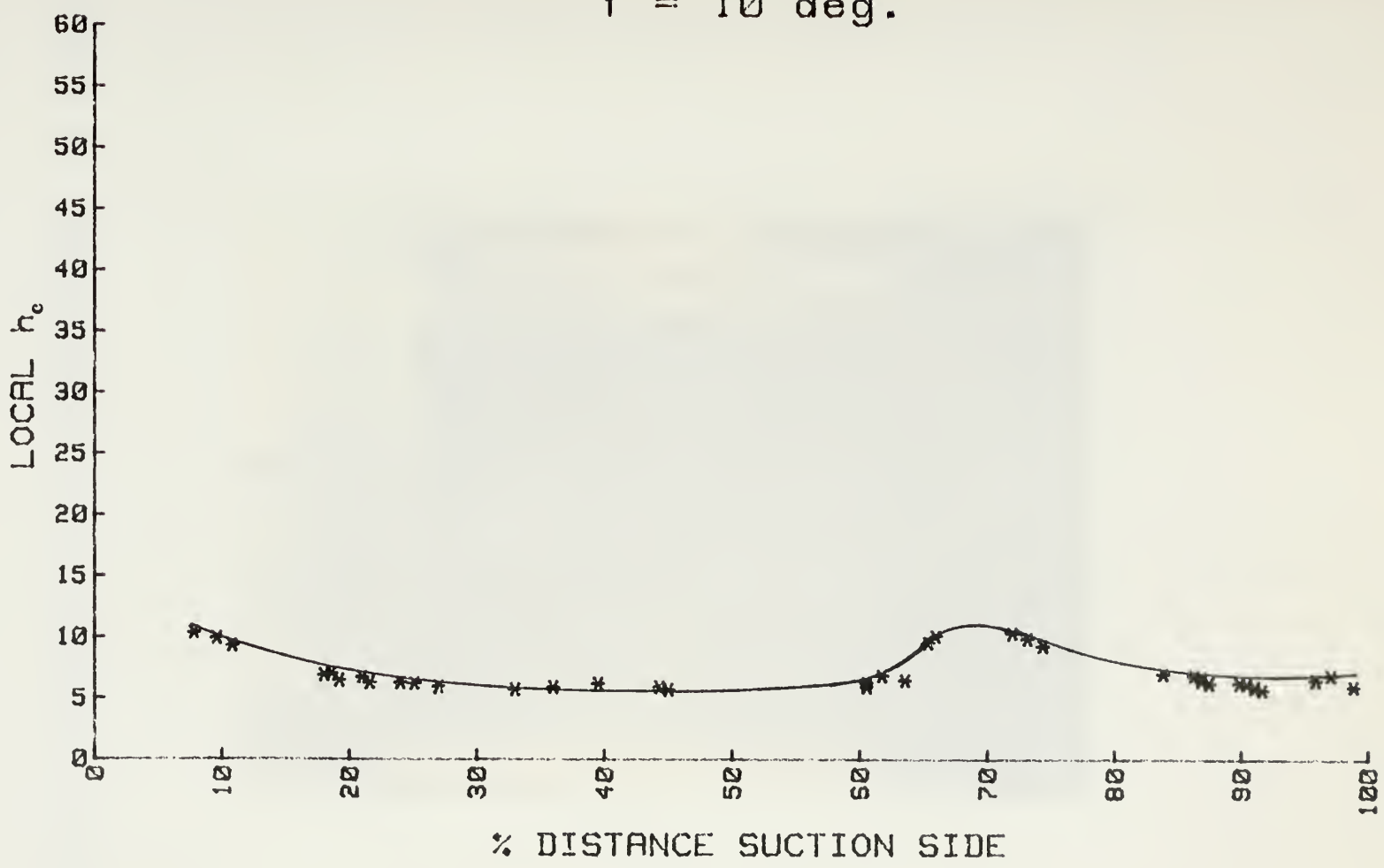


Figure 10. Local convection heat transfer coefficient vs. % of distance from leading edge on suction side of test blade. $Re_c$ = 104,000.

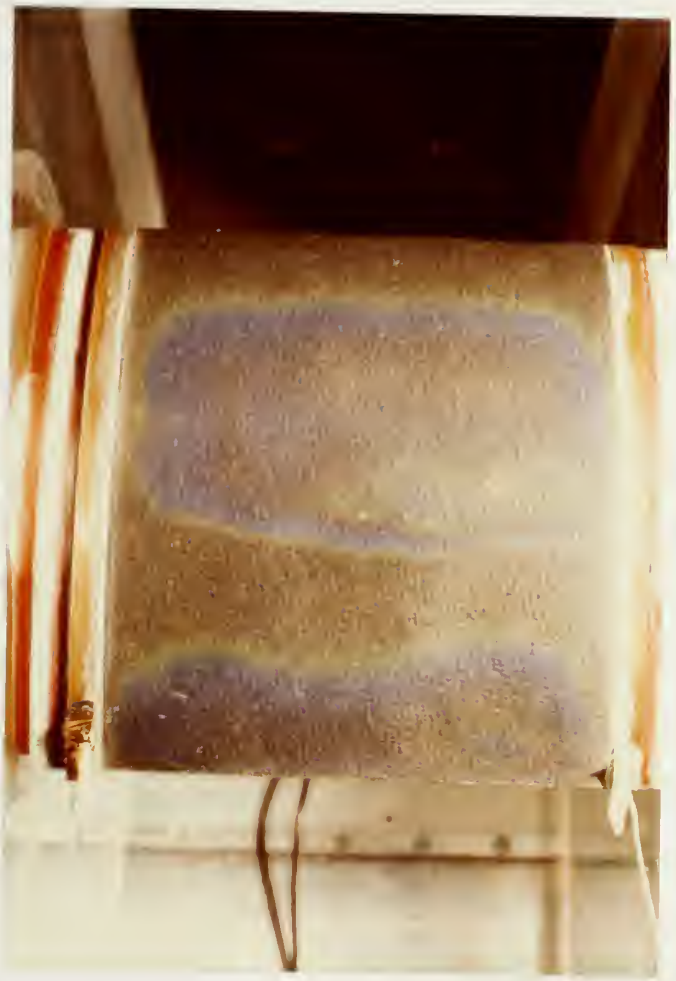

Figure 11. NACA test blade, i = 10 degrees, $Re_c$ = 104,000. Suction side, air flow from top to bottom.

isotherms on the test blade at an angle of incidence of 10 degrees and a Reynolds number of 104,000. The color bands have not yet come together at the 70% distance point which will indicate the cooler part of the blade and the point of flow reattachment.

Again holding the Reynolds number relatively constant ($Re_c$ = 104,000) and increasing the angle of incidence to 25 degrees, a condition is observed that indicates that the blade has passed through its stall angle and the flow is completely separated from the suction side of the blade. As would be expected, Figure 12 shows the values of the heat transfer coefficient to be relatively low. The rise in their values in the mid section and trailing edge areas of the blade, indicate a cooling effect produced by the re-circulating flow in these areas. Figure 13 shows the pattern of isotherms which correspond to this situation.

The observance of the sequences of colors for a particular crystal will give the direction of the temperature gradient. This, along with the discrete temperature information available at any point over the blade surface, enables one to accurately determine the location of the points of interest. Figure 14 compares the local convection heat transfer coefficient distribution for four different Reynolds numbers with the angle of incidence fixed at 15 degrees. Laminar separation occurred at 5% distance from the leading edge for the lowest Reynolds number of 104,000.

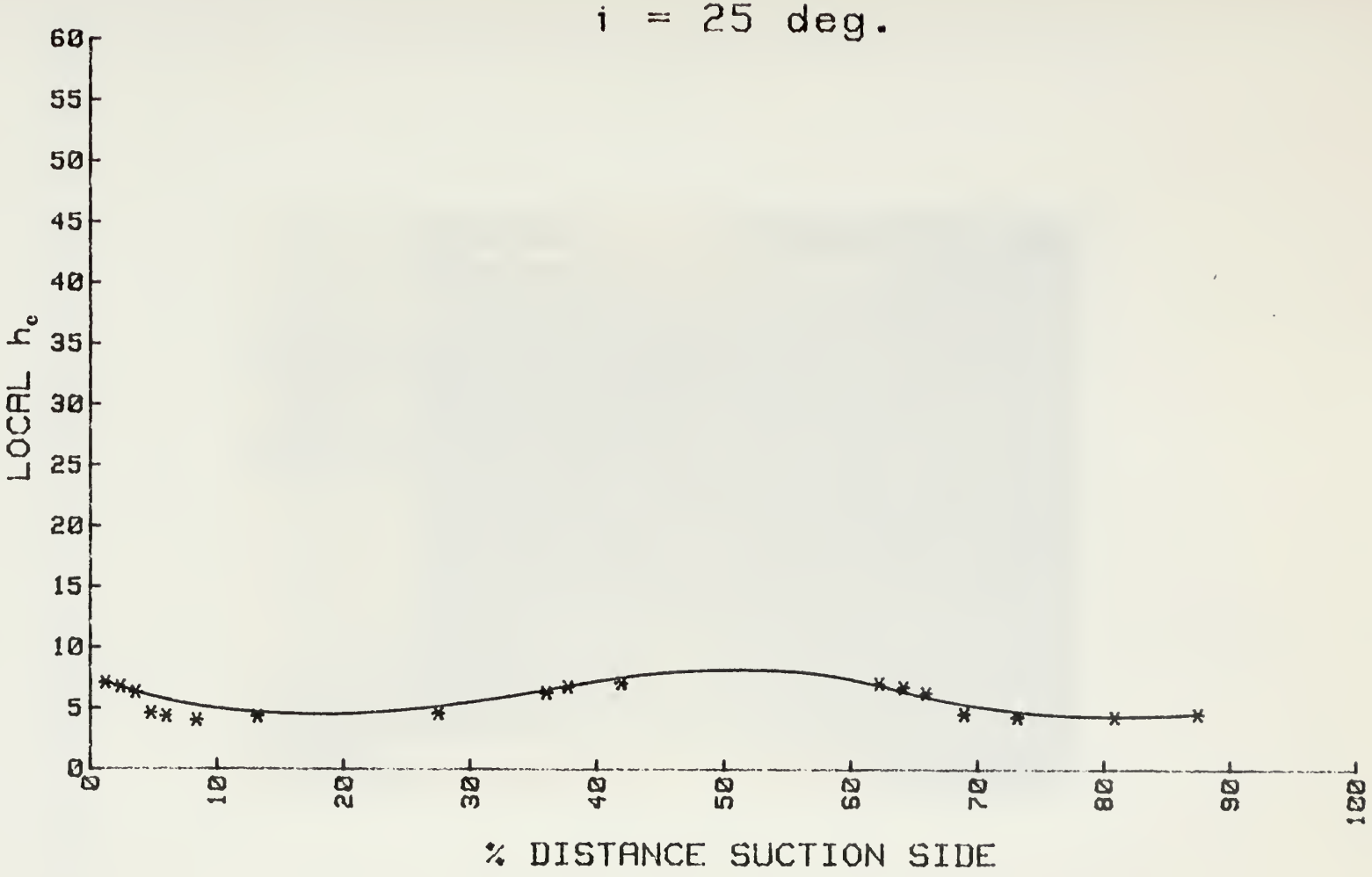


Figure 12. Local convection heat transfer coefficient vs. % of distance from leading edge on suction side of test blade. $Re_c$ = 104,000.

Figure 13. NACA test blade, i = 25 degrees, $Re_c$ = 104,000. Suction side, air flow from top to bottom.

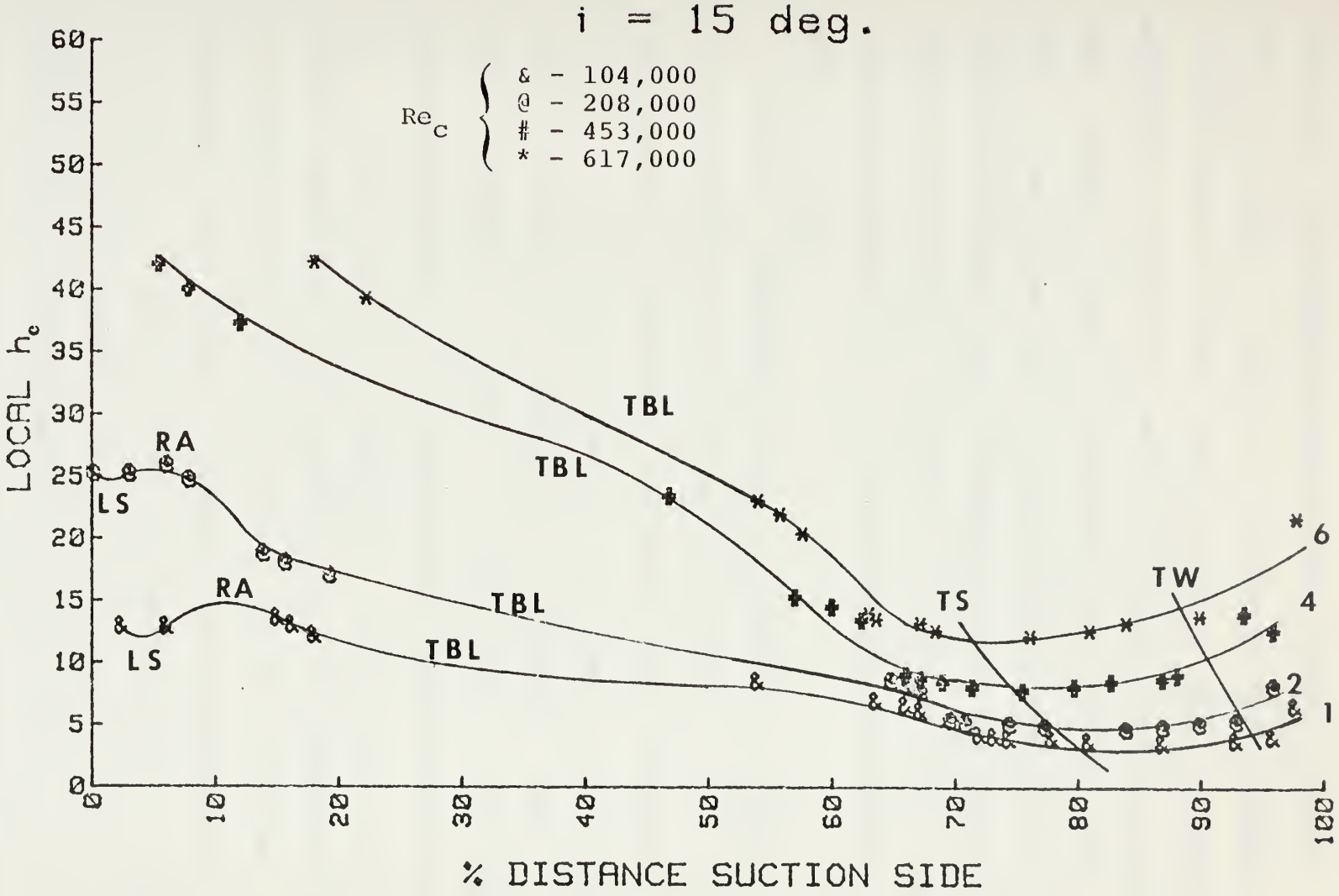


Figure 14. Local convection heat transfer coefficient vs. % of distance from leading edge on suction side of test blade.

This point then moved forward to 2% distance for the Reynolds number of 208,000. For the Reynolds numbers of 454,000 and 617,000 the location of the point of laminar separation, transition, and reattachment was the leading edge. Again for the two lower Reynolds numbers, the first peak in the curves show the reattachment positions. The turbulent boundary layer separation is at the point of lowest heat transfer coefficient value. As can be seen, this occurs from 75% to 85% distance depending on the Reynolds number.

Finally, investigations were conducted at higher Reynolds numbers. By positioning the test blade at 0 degree angle of incidence, increasing the tunnel wind velocity to 100 feet per second, and then rotating the blade to an angle of incidence of 25 degrees, gave a Reynolds number of 414,000. Data was taken in the normal manner between the 60% distance point and the trailing edge. This is shown in Figure 15. In the area from the leading edge back until the 60% point, no temperature data was possible due to the instability of the isotherms. The colors were very erratic, ranging from no color at all to a mixture of all colors in no noticable pattern. Figure 16 is a picture of the test blade in this state, with no isotherms visible in the forward 60% of the blade. It is inferred that the blade was then in a condition of stall in which the fluid was detaching and reattaching to the forward 60% of the suction side of the blade.

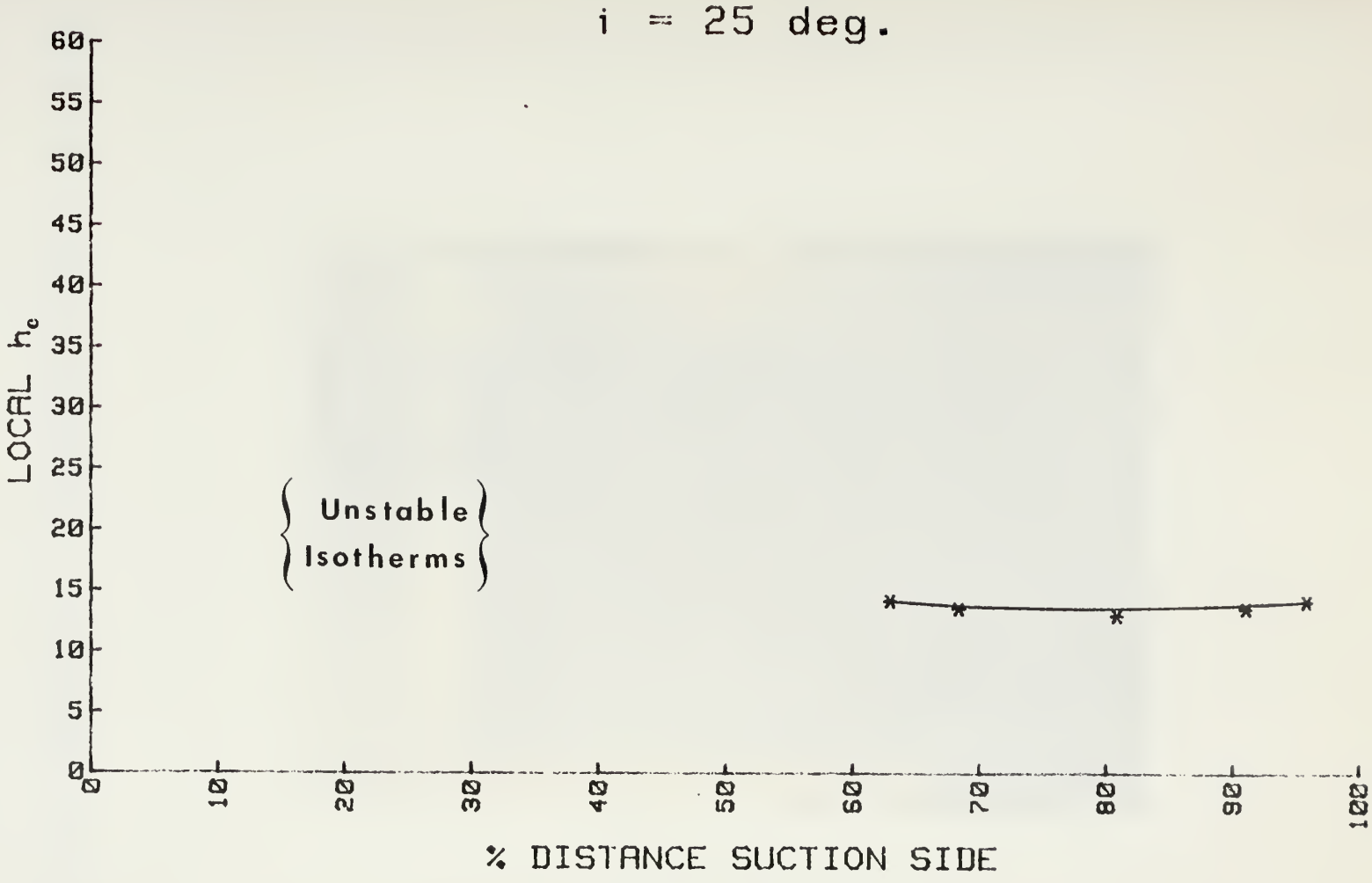


Figure 15. Local convection heat transfer coefficient vs. % of distance from leading edge on suction side of test blade. $Re_c$ = 414,000.

Figure 16. NACA test blade, i = 25 degrees, $Re_c$ = 414,000. Suction side, air flow from top to bottom.

The blade was then returned to an angle of 0 degree, and the air speed further increased to 150 feet per second. The blade was rotated to an angle of incidence of 5 degrees for a Reynolds number of 614,000. Figure 17 shows the isotherms of the fluid with the blade in this condition. These isotherms can be seen at the leading edge and between the 50% distance point to the trailing edge, and were of the usual pattern, perpendicular to the direction of flow. From just after the leading edge to the 50% distance point, isotherms were seen parallel to the direction of flow. This area should be observed with a flow visualization technique such as smoke to verify their actual existence on the suction side of the test blade. The actual presence of such a complex three-dimensional flow could be the subject of further studies.

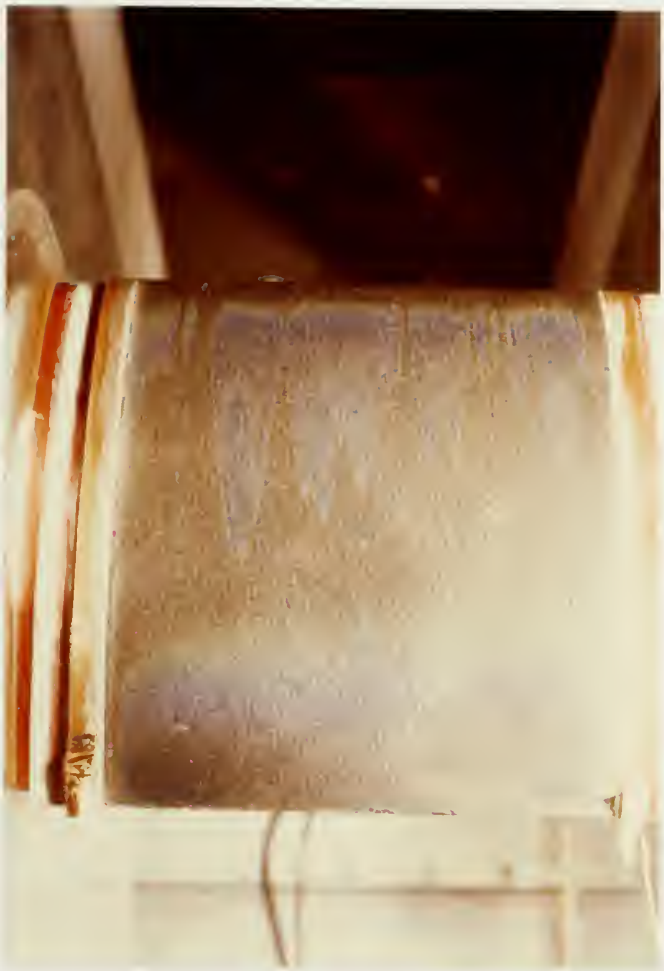

Figure 17. NACA test blade, i = 5 degrees, $Re_c$ = 614,000. Suction side, air flow from top to bottom.

## V. CONCLUSIONS AND RECOMMENDATIONS

The liquid crystal thermography studied in this investigation shows that it's use will provide an excellent technique to obtain both quantitative and qualitative heat transfer information on heated objects placed in a forced convective environment. It was possible to quickly reduce the data to obtain information as to the convection heat transfer coefficient as it varied over the entire suction side of the compressor blade. From the values of the heat transfer coefficient, the character of the flow was easily determined. The location of separation point, reattachment point, separation bubbles, and stall angle were able to be determined. With adjustments in the voltage supplied to the temsheet, a continuous picture was seen, which is very advantageous as compared to pressure taps or thermocouples, which provide information only at discrete points. This continuous coverage enabled the viewing of the isotherms that were produced parallel to the direction of flow, particularly on the pressure side of the blade.

The ability to observe the isotherms could be made easier if blades in the future would be mounted in a vertical position, with a viewing window to see both sides of the blade. To study the flow over a particular blade shape, the thickness of the temsheet would have to be

considered. A blade built to allow the temsheet to be installed in a recessed area with the surface of the temsheet conforming to the blade specifications, made from a material with a known value of the thermal conductivity, would improve the usefulness of the data. An accurate value of the thermal conductivity of temsheet should also be determined, if this material is to be used for future investigations. If information is needed at higher Reynolds numbers or at a greater angle of incidence, a low numbered crystal should be used, due to the voltage limitations of the equipment.

As a final recommendation, prior to investigating the flow over the compressor blade in a cascade wind tunnel, the type of flow inferred from the convection heat transfer coefficient should be viewed with some type of flow visualization technique in the subsonic wind tunnel.

## APPENDIX A

## ELECTRICAL POWER REQUIREMENT FOR LIQUID CRYSTAL THERMOGRAPHY

Turbulent flow of air is assumed over a "flat plate" with a span of ten inches and a chord length of eight inches. Surface area equals 160 square inches. Plate surface temperature to be 100 degrees Fahrenheit. Air flow equals 275 feet per second at 65 degrees Fahrenheit.

$$T_f = \frac{T_b + T_\infty}{2} = \frac{100+65}{2} = 82.5°F$$

Air properties at 82.5°F:

$$\mu = 0.04797 \frac{lbm}{hr\text{-}ft}$$

$$k = 0.0152 \frac{Btu}{hr\text{-}ft\text{-}°F}$$

$$Pr = 0.708$$

$$\rho = 0.0735 \frac{lbm}{ft^3}$$

$$\nu = 1.8126 \times 10^{-4} \frac{ft^2}{sec}$$

$$C_p = 0.240 \frac{Btu}{lbm\text{-}°F}$$

The above conditions give:

$$Re_c = \frac{\rho u_\infty c}{\mu} = 1.011 \times 10^6$$

For turbulent flow, to find the average convective heat transfer coefficient, equation 5-81 of Ref. 13 is used:

$$\bar{N}u_L = \frac{\bar{h}L}{k} = Pr^{1/3} (0.037Re_L^{0.8} - 850)$$

$$\frac{\bar{h}L}{k} = 1341.85$$

$$h = 30.59 \frac{Btu}{hr\text{-}ft^2\text{-}^\circ F}$$

Equating the heat generated in the test blade by the electrical current to the heat removed by forced convection (heat loss by radiation was considered negligible) gives:

$$Power = I^2R = \bar{h}A(T_b - T_\infty) = VI$$

which leads to

$$I_{min} = \frac{\bar{h}A(T_b - T_\infty)}{V_{max}} = \frac{P}{V_{max}}$$

and

$$R_{max} = \frac{\bar{h}A(T_b - T_\infty)}{I^2_{min}} = \frac{P}{I^2_{min}}$$

The power required to heat the blade is calculated as

$$P = \bar{h}A(T_b - T_\infty) = 349 \text{ watts}$$

For a power supply rated at a maximum output potential of 60 volts, current and resistance requirements are:

$$I_{min} = 5.8 \text{ amps}$$

$$R_{max} = 10.3 \text{ ohms}$$

APPENDIX B

LIQUID CRYSTAL CALIBRATION RESULTS

| Liquid Crystal (NCR Designation) | Color Transition | | |
|---|---|---|---|
| | Red (°F) | Green (°F) | Blue (°F) |
| R-33 | 91.4 | 92.5 | 94.2 |
| S-40 | 104.1 | 105.2 | 106.3 |
| R-45 | 106.6 | 108.2 | 109.5 |

# APPENDIX C

## BLADE EDGE EFFECTS

### A. SIDE WALLS

To eliminate any readings that could be affected by the boundary layer caused by flow pass the two side walls, the boundary layer thickness was calculated for a "worst case" situation.

Assume fully turbulent boundary layer, equation 5-85 of Ref. 13 is used:

$$\frac{\delta}{X} = 0.381\ Re_x^{-1/5}$$

which leads to

$$\delta = 0.381 X^{4/5} \left(\frac{\rho u_\infty}{\mu}\right)^{-1/5}$$

for $\rho = 0.0735\ \frac{lbm}{ft}$

$\mu = 0.04797\ \frac{lbm}{hr\text{-}ft}$

$u_\infty = 50\ \frac{ft}{sec}$

$$\delta = 0.031 X^{4/5} \text{ inches}$$

for X (distance from leading edge of side wall to trailing edge of blade) equal to 16 inches

$\delta = 0.286$ inches

$Re_x = 368{,}000.$

B. TEST BLADE

The span wise variation in the temperature field due to end losses was estimated by treating the temsheet as a thin fin. Symmetry about the centerline was assumed. A "worst case" situation was also assumed with the temperature at the outer edge of the temsheet equal to the free stream temperature, $T_\infty$. Using the equation developed in Ref. 5:

$$\frac{T-T_\infty}{T_o-T_\infty} = \left(1 - \frac{\text{Cosh}(my)}{\text{Cosh}(mL)}\right)$$

where

$y$ = distance from centerline

$L$ = distance from centerline to outer edge

$T$ = temperature at location $y$

$(T_o - T_\infty)$ = centerline temperature excess

$$m = \left[\frac{h}{kt}\right]^{1/2}$$

$t$ = thickness of test section material

$k$ = thermal conductivity of test section material

$h$ = surface heat transfer coefficient

$T_\infty$ = free stream air temperature

The boundary conditions used for the problem were

at $y = 0$, $\frac{dT}{dy} = 0$

at $y = L$, $T = T_\infty$

Using representative values of:

$$h = 5 \frac{Btu}{hr\text{-}ft^2\text{-}^\circ F} \qquad \text{[Ref. 5]}$$

$$k = 0.06 \frac{Btu}{hr\text{-}ft\text{-}^\circ F} \qquad \text{[Ref. 5]}$$

$t = 0.039$ inches

$2L = 8$ inches

The distance y for which $(\frac{T-T_\infty}{T_o-T_\infty}) = 0.99$ was found to be 3.65 inches. Figure 18 shows the final placement of the temsheet and copper strips on the test blade.

It was concluded that if the electrodes were spaces 8 inches apart and 1 inch from the ends of the blade, using only the center 7 inches, would yield temperature information that was essentially uninfluenced by effects from the turbulent boundary layer developed by the side walls and heat lost through the edges of the temsheet.

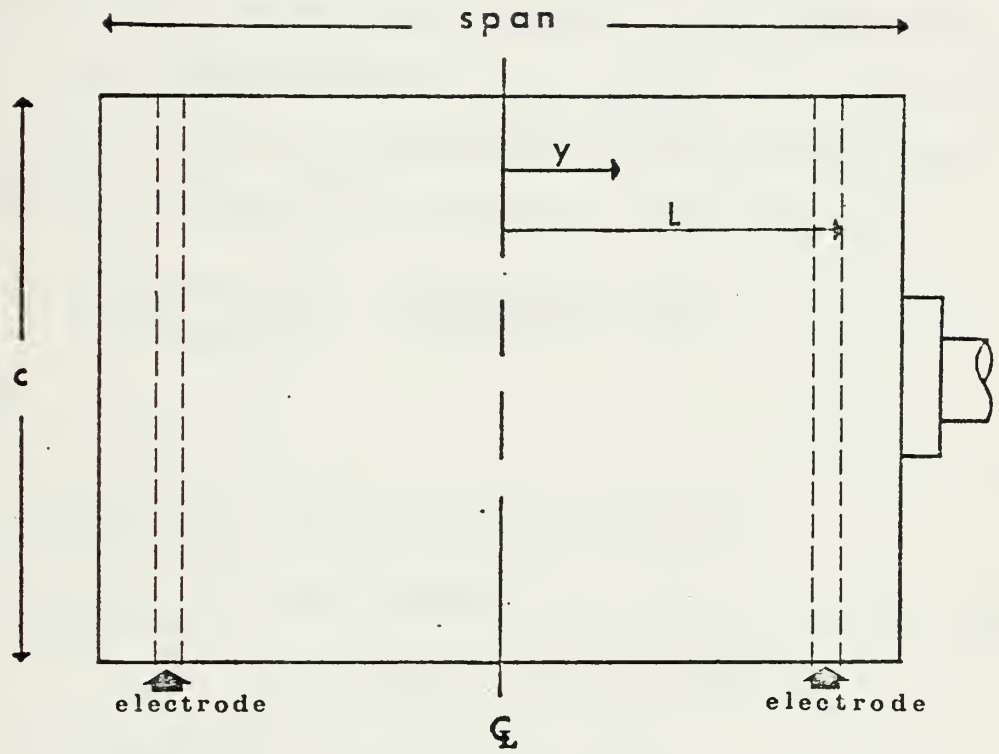


Figure 18. Placement of temsheet and copper strips (electrodes) on the test blade.

## APPENDIX D

## DATA AND DATA REDUCTION

In order to experimentally determine the convection heat transfer coefficient as a function of location on the suction side of the blade, measured from the leading edge, a relationship between the surface heat flux produced by the Joulean heating effect in the temsheet and the losses through radiation and conduction had to be established. Performing a simple heat balance on the blade gives

$$h_c = \frac{Q_{electrical}}{\Delta TA_{temsheet}} - \frac{Q_{conduction}}{\Delta TA_s} - h_r$$

where

$Q_{electrical}$ = Heat transfer into blade

$Q_{conduction}$ = Heat transfer loss through the two ends not covered by the temsheet

$h_r$ = Radiation heat transfer coefficient

$= [\sigma F_{1-2}(T+T_\infty)(T^2+T_\infty^2)]$

$F_{1-2}$ = Radiation exchange factor between the test blade and its surroundings

$\sigma$ = Stefan-Boltzman constant

$A_s$ = surface area of the short end fins

The electrical heat transfer value was determined by

$$Q_{electrical} = \frac{V^2}{R}$$

The conduction losses through the two blade ends were estimated by modeling the ends as short fins, with convection end losses. A value of $\bar{h}$ was estimated using the average of the $h_c$ calculated without the conduction loss factor for the Reynolds number and angle of incidence of the blade. Using case "2" from Ref. 13 (fin of finite length and losses) by convection from its end)

$$Q_{conduction} = [\bar{h}(B_p)kA_p]^{\frac{1}{2}} (\Delta T) \frac{\sinh(mL) + \frac{(\frac{h}{mk})}{\cosh(mL)}}{\cosh(mL) + \frac{(\frac{h}{mk})}{\sinh(mL)}} A_s$$

where

$\bar{h}$ = average convection heat transfer coefficient for the short end fins

$B_p$ = blade profile perimeter

$k$ = thermal conductivity of the test blade

$A_p$ = profile area of the test blade

$\Delta T = T - T_\infty$

$$m = \left[ \frac{\bar{h}B_p}{kA_p} \right]^{\frac{1}{2}}$$

$L$ = length of the short fin

$A_s$ = surface area of the short fin

A sample calculation is provided for illustration using the following values from the data at a Reynolds number of 208,000, a 15 degree angle of incidence, and 7.0 inches from the leading edge on the suction side of the blade:

$V = 31.45$ volts

$R = 11.5$ ohms

$B_p = 16.1$ inches

$k = 0.2 \ \frac{Btu}{hr\text{-}ft\text{-}^\circ F}$

$T = 109.5^\circ F$

$T_\infty = 60.8^\circ F$

$A_p = 4.6 \ in^2$

$A_s = 16.6 \ in^2$

$L = 1$ inch

$t = 0.75$ inch

$\sigma = 0.1714 \times 10^{-8} \ \frac{Btu}{hr\text{-}ft^2\text{-}^\circ R^4}$

$F_{1\text{-}2} = 1.0$

$\bar{h} = 16 \ \frac{Btu}{hr\text{-}ft^2\text{-}^\circ F}$

$mL = 16.99$

$h_r = 1.11 \ \frac{Btu}{hr\text{-}ft^2\text{-}^\circ F}$

$Q_{electrical} = 293.46 \ \frac{Btu}{hr}$

$Q_{conduction} = 2.11 \ \frac{Btu}{hr}$ (for each end)

$h_c = 6.57 \ \frac{Btu}{hr\text{-}ft^2\text{-}^\circ F} - 0.752 \ \frac{Btu}{hr\text{-}ft^2\text{-}^\circ F} - 1.11 \ \frac{Btu}{hr\text{-}ft^2\text{-}^\circ F}$

$h_c = 4.71 \ \frac{Btu}{hr\text{-}ft^2\text{-}^\circ F}$

The data sheets for all four Reynolds numbers investigated at an angle of incidence of 15 degrees follow.

DATA

Air Speed 0.25 in $H_2O$ i angle 15 degrees

25 ft/sec $\bar{h}$ 10.0 $\frac{Btu}{hr\text{-}ft^2\text{-}°F}$

$Re_c$ 104,000 $P_{atm}$ 30.07 in Hg

| V | R | Cry. | Color | Temp. (°F) | Location (in) | (%) | $T_\infty$ | $\Delta T$ | Uncorr $h_c$ | $h_r$ | Corr $h_c$ |
|---|---|---|---|---|---|---|---|---|---|---|---|
| 27.77 | 11.6 | R-33 | R | 91.4 | 5.3 | 63.5 | 63.0 | 28.4 | 8.71 | 1.06 | 7.05 |
| 27.77 | 11.6 | R-33 | G | 92.5 | 5.5 | 65.9 | 63.0 | 29.5 | 8.39 | 1.07 | 6.73 |
| 27.77 | 11.6 | R-33 | B | 94.2 | 5.6 | 67.1 | 63.0 | 31.2 | 7.93 | 1.07 | 6.26 |
| 27.77 | 11.6 | S-40 | R | 104.1 | 6.0 | 71.9 | 63.0 | 41.1 | 6.02 | 1.10 | 4.32 |
| 27.77 | 11.6 | S-40 | G | 105.2 | 6.1 | 73.1 | 63.0 | 42.2 | 5.86 | 1.11 | 4.16 |
| 27.77 | 11.6 | S-40 | B | 106.3 | 6.2 | 74.3 | 63.0 | 43.3 | 5.71 | 1.11 | 4.01 |
| 27.77 | 11.6 | R-45 | R | 106.6 | 6.5 | 77.8 | 63.0 | 43.6 | 5.68 | 1.11 | 4.04 |
| 27.77 | 11.6 | R-45 | G | 108.2 | 6.75 | 80.8 | 63.0 | 45.2 | 5.47 | 1.12 | 3.76 |
| 27.77 | 11.6 | R-45 | B | 109.5 | 7.25 | 86.8 | 63.0 | 46.5 | 5.32 | 1.12 | 3.61 |
| 27.77 | 11.6 | R-45 | G/R | 107.4 | 7.75 | 92.8 | 63.0 | 44.4 | 5.57 | 1.11 | 3.87 |
| 27.77 | 11.6 | S-40 | B/G/R | 105.2 | 8.0 | 95.8 | 63.0 | 42.2 | 5.86 | 1.11 | 4.16 |
| 27.77 | 11.6 | R-33 | B/G/R | 92.8 | 8.15 | 97.6 | 63.0 | 29.8 | 8.30 | 1.07 | 6.64 |
| 36.85 | 11.6 | R-33 | R | 91.4 | 1.25 | 15.0 | 63.0 | 28.4 | 15.34 | 1.06 | 13.68 |
| 36.85 | 11.6 | R-33 | G | 92.5 | 1.35 | 16.2 | 63.0 | 29.5 | 14.77 | 1.07 | 13.11 |
| 36.85 | 11.6 | R-33 | B | 94.2 | 1.5 | 18.0 | 63.0 | 31.2 | 13.97 | 1.07 | 12.30 |
| 36.85 | 11.6 | S-40 | C | 105.2 | 4.5 | 53.9 | 63.0 | 42.2 | 10.32 | 1.11 | 8.62 |
| 36.85 | 11.6 | R-33 | B/G/R | 92.8 | 0.5 | 6.0 | 63.0 | 29.8 | 14.62 | 1.07 | 12.96 |
| 36.85 | 11.6 | R-33 | R/G/B | 92.8 | 0.2 | 2.4 | 63.0 | 29.8 | 14.62 | 1.07 | 12.96 |

DATA

Air Speed 0.5 in $H_2O$

50 ft/sec

$Re_c$ 208,000

i Angle 15 degrees

$\bar{h}$ 15.0 $\frac{Btu}{hr\text{-}ft^2\text{-}°F}$

$P_{atm}$ 24.99 in Hg

| V | R | Cry. | Color | Temp. (°F) | Location (in) | (%) | T∞ | ΔT | Uncorr $h_c$ | $h_r$ | Corr $h_c$ |
|---|---|---|---|---|---|---|---|---|---|---|---|
| 31.45 | 11.5 | R-33 | R | 91.4 | 5.4 | 64.7 | 60.8 | 30.6 | 10.46 | 1.06 | 8.68 |
| 31.45 | 11.5 | R-33 | G | 92.5 | 5.5 | 65.9 | 60.8 | 31.7 | 10.10 | 1.06 | 8.31 |
| 31.45 | 11.5 | R-33 | B | 94.2 | 5.6 | 67.1 | 60.8 | 33.4 | 9.58 | 1.07 | 7.79 |
| 31.45 | 11.5 | S-40 | R/G | 104.7 | 5.8 | 69.5 | 60.8 | 43.9 | 7.29 | 1.10 | 5.47 |
| 31.45 | 11.5 | S-40 | G/B | 105.8 | 5.9 | 70.7 | 60.8 | 45.0 | 7.11 | 1.10 | 5.28 |
| 31.45 | 11.5 | R-45 | R | 106.6 | 6.2 | 74.3 | 60.8 | 45.8 | 6.99 | 1.10 | 5.16 |
| 31.45 | 11.5 | R-45 | G | 108.2 | 6.45 | 77.2 | 60.8 | 47.4 | 6.75 | 1.11 | 4.92 |
| 31.45 | 11.5 | R-45 | B | 109.5 | 7.0 | 83.8 | 60.8 | 48.7 | 6.57 | 1.11 | 4.73 |
| 31.45 | 11.5 | R-45 | G | 108.2 | 7.25 | 86.8 | 60.8 | 47.4 | 6.75 | 1.11 | 4.92 |
| 31.45 | 11.5 | R-45 | R | 106.6 | 7.50 | 89.8 | 60.8 | 45.8 | 6.99 | 1.10 | 5.16 |
| 31.45 | 11.5 | S-40 | B/G/R | 105.2 | 7.75 | 92.8 | 60.8 | 44.4 | 7.21 | 1.10 | 5.38 |
| 31.45 | 11.5 | R-33 | B/G/R | 92.8 | 8.0 | 95.8 | 60.8 | 32.0 | 10.0 | 1.06 | 8.21 |
| 44.31 | 11.5 | R-33 | R | 91.4 | 1.15 | 13.8 | 60.6 | 30.8 | 20.63 | 1.06 | 18.85 |
| 44.31 | 11.5 | R-33 | G | 92.5 | 1.3 | 15.6 | 60.6 | 31.9 | 19.92 | 1.06 | 18.13 |
| 44.31 | 11.5 | R-33 | B | 94.2 | 1.6 | 19.2 | 60.8 | 33.6 | 18.91 | 1.07 | 17.12 |
| 51.7 | 11.5 | R-33 | R/G | 92.0 | 0.5 | 6.0 | 60.8 | 31.2 | 27.73 | 1.06 | 25.94 |
| 51.7 | 11.5 | R-33 | G/B | 93.4 | 0.65 | 7.8 | 60.8 | 32.6 | 26.54 | 1.06 | 24.75 |
| 51.7 | 11.5 | R-33 | R/G/B | 92.8 | 0.05 | 0.1 | 60.8 | 32.0 | 27.03 | 1.06 | 25.24 |
| 51.7 | 11.5 | R-33 | B/G/R | 92.8 | 0.25 | 3.0 | 60.8 | 32.0 | 27.03 | 1.06 | 25.24 |

DATA

Air Speed 2.6 in $H_2O$
110 ft/sec

i Angle 15 degrees

$\bar{h}$ 25 $\frac{Btu}{hr\text{-}ft^2\text{-}°F}$

$Re_c$ 454,000

$P_{atm}$ 30.09 in Hg

| V | R | Cry. | Color | Temp. (°F) | Location (in) | (%) | $T_\infty$ | $\Delta T$ | Uncorr $h_c$ | $h_r$ | Corr $h_c$ |
|---|---|---|---|---|---|---|---|---|---|---|---|
| 36.07 | 11.7 | R-33 | R | 91.4 | 4.75 | 56.9 | 67.6 | 23.8 | 17.39 | 1.08 | 15.37 |
| 36.07 | 11.7 | R-33 | G | 92.5 | 5.0 | 59.9 | 67.6 | 24.9 | 16.62 | 1.08 | 14.60 |
| 36.07 | 11.7 | R-33 | B | 94.2 | 5.2 | 62.3 | 67.6 | 26.6 | 15.56 | 1.09 | 13.53 |
| 36.07 | 11.7 | S-40 | R/G | 104.7 | 5.5 | 65.9 | 67.6 | 37.1 | 11.16 | 1.12 | 9.10 |
| 36.07 | 11.7 | S-40 | G/B | 105.8 | 5.6 | 67.1 | 67.6 | 38.2 | 10.83 | 1.12 | 8.77 |
| 36.07 | 11.7 | R-45 | R | 106.6 | 5.75 | 68.9 | 67.6 | 39.0 | 10.61 | 1.12 | 8.55 |
| 36.07 | 11.7 | R-45 | G | 108.2 | 5.95 | 71.3 | 67.6 | 40.6 | 10.19 | 1.13 | 8.13 |
| 36.07 | 11.7 | R-45 | B | 109.5 | 6.3 | 75.4 | 67.6 | 41.9 | 9.88 | 1.13 | 7.80 |
| 36.07 | 11.7 | R-45 | G | 108.2 | 6.65 | 79.6 | 67.6 | 40.6 | 10.19 | 1.13 | 8.13 |
| 36.07 | 11.7 | R-45 | R | 106.6 | 6.9 | 82.6 | 67.6 | 39.0 | 10.61 | 1.12 | 8.55 |
| 36.07 | 11.7 | S-40 | B/G | 105.8 | 7.25 | 86.8 | 67.6 | 38.2 | 10.83 | 1.12 | 8.77 |
| 36.07 | 11.7 | S-40 | G/R | 104.7 | 7.35 | 88.0 | 67.6 | 37.1 | 11.16 | 1.12 | 9.10 |
| 36.07 | 11.7 | R-33 | B/G | 93.4 | 7.8 | 93.4 | 67.6 | 25.8 | 16.04 | 1.08 | 14.02 |
| 36.07 | 11.7 | R-33 | G/R | 92.0 | 8.0 | 95.8 | 67.6 | 24.4 | 16.96 | 1.09 | 12.65 |
| 56.7 | 11.7 | R-33 | R | 91.7 | 0.45 | 5.4 | 68.2 | 23.8 | 44.08 | 1.08 | 42.06 |
| 56.7 | 11.7 | R-33 | G | 92.5 | 0.65 | 7.8 | 68.2 | 24.3 | 42.09 | 1.08 | 40.07 |
| 56.7 | 11.7 | R-33 | B | 94.2 | 1.0 | 12.0 | 68.2 | 26.0 | 39.34 | 1.09 | 37.31 |
| 56.7 | 11.7 | R-45 | G | 108.2 | 3.9 | 46.7 | 68.2 | 40.0 | 25.57 | 1.13 | 23.50 |

DATA

Air Speed 5.0 in $H_2O$

150 ft/sec

i Angle 15 degrees

$\bar{h}$ 30 $\frac{Btu}{hr\text{-}ft^2\text{-}^\circ F}$

$Re_c$ 617,000

$P_{atm}$ 30.02 in Hg

| V | R | Cry. | Color | Temp. (°F) | Location (in) | Location (%) | $T_\infty$ | $\Delta T$ | Uncorr $h_c$ | $h_r$ | Corr $h_c$ |
|---|---|---|---|---|---|---|---|---|---|---|---|
| 43.1 | 11.5 | R-33 | R | 91.4 | 4.5 | 53.9 | 67.6 | 23.8 | 25.26 | 1.08 | 23.15 |
| 43.1 | 11.5 | R-33 | G | 92.5 | 4.65 | 55.7 | 67.6 | 24.9 | 24.15 | 1.08 | 22.04 |
| 43.1 | 11.5 | R-33 | B | 94.2 | 4.8 | 57.5 | 67.6 | 26.6 | 22.60 | 1.09 | 20.49 |
| 43.1 | 11.5 | S-40 | R/G | 104.7 | 5.25 | 62.9 | 67.6 | 37.1 | 16.21 | 1.12 | 14.06 |
| 43.1 | 11.5 | S-40 | G/R | 105.8 | 5.3 | 63.5 | 67.6 | 38.2 | 15.74 | 1.12 | 13.59 |
| 43.1 | 11.5 | R-45 | R | 106.6 | 5.6 | 67.1 | 67.6 | 39.0 | 15.42 | 1.12 | 13.26 |
| 43.1 | 11.5 | R-45 | G | 108.2 | 5.7 | 68.3 | 67.6 | 40.6 | 14.81 | 1.13 | 12.65 |
| 43.1 | 11.5 | R-45 | B | 109.5 | 6.35 | 76.0 | 67.6 | 41.9 | 14.35 | 1.13 | 12.19 |
| 43.1 | 11.5 | R-45 | G | 108.2 | 6.75 | 80.8 | 67.6 | 40.1 | 14.81 | 1.13 | 12.65 |
| 43.1 | 11.5 | R-45 | R | 106.6 | 7.0 | 83.8 | 67.6 | 39.0 | 15.42 | 1.12 | 13.26 |
| 43.1 | 11.5 | S-40 | B/G/R | 105.2 | 7.5 | 89.8 | 67.6 | 37.6 | 15.99 | 1.12 | 13.84 |
| 43.1 | 11.5 | R-33 | B/G/R | 92.8 | 8.15 | 97.6 | 67.6 | 25.2 | 23.86 | 1.08 | 21.75 |
| 57.71 | 11.5 | R-33 | G | 92.5 | 1.5 | 18.0 | 68.2 | 24.3 | 44.36 | 1.08 | 42.25 |
| 57.71 | 11.5 | R-33 | B | 94.2 | 1.85 | 22.2 | 68.2 | 26.0 | 41.45 | 1.09 | 39.34 |

# APPENDIX E

## UNCERTAINTY ANALYSIS

The uncertainties for the final results were calculated using the method of Kline and McClintock described in Ref. 14. The measured variables which were the origins of uncertainty were voltage, resistance, free stream air temperature, blade surface temperature, free stream air velocity, atmospheric conditions, angle of incidence, isotherm location, and blade physical measurements.

### THE REYNOLDS NUMBER

The Reynolds numbers were calculated from

$$Re_c = \frac{uc}{\nu}$$

$$\frac{\Delta Re_c}{Re_c} = \left[ \left(\frac{\Delta \nu}{\nu}\right)^2 + \left(\frac{\Delta c}{c}\right)^2 + \left(\frac{\Delta u}{u}\right)^2 \right]^{1/2}$$

For the experimental run at a free stream velocity of 25 feet per second

$$\nu = 1.6 \times 10^{-4} \pm 0.1 \times 10^{-4} \ \frac{ft^2}{sec}$$

$$c = 0.67 \pm 0.01 \text{ ft}$$

$$u = 25 \pm 10\% \ \frac{ft}{sec}$$

$$\frac{\Delta Re_c}{Rec} = \left[ \left( \frac{0.1 \times 10^{-4}}{1.6 \times 10^{-4}} \right)^2 + \left( \frac{0.01}{0.67} \right)^2 + \left( \frac{2.5}{25} \right)^2 \right]^{1/2}$$

$$\frac{\Delta Re_c}{Re_c} = 0.119$$

with $Re_c = 105,000$ $\Delta Re_c = 12,000$

The values of the uncertainties for the results are listed below for a Reynolds number of 105,000 and an angle of incidents of 0 degrees.

| Quantity | Uncertainty |
|---|---|
| $h_r$ | 9.2% |
| $Q_{conduction}$ | 17.7% |
| $Q_{electrical}$ | 0.9% |
| $h_c$ | 20.0% |

The values of the uncertainties for the measured variables are listed below.

| Quantity | Uncertainty |
|---|---|
| V | 0.01 volts |
| R | 0.1 ohms |
| $T_\infty$ | 0.2°F |
| x (isotherm location) | 0.1 inch |
| $T_b$ at x | 0.1°F |
| i | 1.0 degree |
| $P_{atm}$ | 0.01 in. Hg |
| u | 10% |

# LIST OF REFERENCES


1. Air Force Aero Propulsion Laboratory Report AFAPL-TR-78-52, The Aerothermodynamics of Aircraft Gas Turbine Engines, by Oates, G. C., and others, July 1978.

2. Cooper, T. E., Field, R. J., and Meyer, J. F., "Liquid Crystal Thermography and Its Application to Convective Heat Transfer," Journal of Heat Transfer, V. 97, No. 3, pp. 442-450, August 1975.

3. Petrovic, W. K., An Experimental Investigation of the Temperature Field Produced by a Surgical Cryoprobe, MSME Thesis, U.S. Naval Postgraduate School, Monterey, California, 1972.

4. Meyer, J. F., An Experimental Investigation of the Heat Transfer Characteristics of a Heated Cylinder Placed in a Cross Flow of Air, ENGR Thesis, U.S. Naval Postgraduate School, Monterey, California, 1973.

5. Field, R. J., Liquid Crystal Mapping of the Surface Temperature on a Heated Cylinder Placed in a Crossflow of Air, MSME Thesis, U.S. Naval Postgraduate School, Monterey, California, 1974.

6. Durao, M. C., Investigation of Heat Transfer in Straight and Curved Rectangular Ducts Using Liquid Crystal Thermography, ENGR Thesis, U.S. Naval Postgraduate School, Monterey, California, 1977.

7. Dzung, L. S., Flow Research on Blading, Proceedings of the Symposium on Flow Research on Blading, pp. 243-274 and pp. 322-371, Elsevier Publishing Company, New York, 1970.

8. Scholz, D. N., Aerodynamics of Cascades, Advisory Group for Aerospace Research and Development, 1977.

9. Smith, L. H., Aerodynamic Characteristics of an Axisymmetric Body Undergoing a Uniform Pitching Motion, Ph.D. Thesis, U.S. Naval Postgraduate School, Monterey, California, 1974.

10. Miller, W. R., Hot Wire Anemometer Investigation of Turbulence Levels and Development of Liquid Crystal Flow Visualization Techniques for the Rectilinear Cascade Test Facility, MSME Thesis, U.S. Naval Postgraduate School, Monterey, California, 1979.

11. Roshko, A., "Experiments on the Flow Past a Circular Cylinder at Very High Reynolds Numbers," Journal of Fluid Mechanics, V. 10, pp. 345-356, May 1961.

12. Roberts, W. B., The Effect of Reynolds Number and Laminar Separation on Axial Cascade Performance, Paper Presented at Gas Turbine Conference, Zurich, Switzerland, 31 Mar 74.

13. Holman, J. P., Heat Transfer, 4th Ed., McGraw-Hill, 1976.

14. Holman, J. P., Experimental Methods for Engineers, 3rd Ed., McGraw-Hill, 1978.

INITIAL DISTRIBUTION LIST

| | | No. Copies |
|---|---|---|
| 1. | Defense Technical Information Center<br>Cameron Station<br>Alexandria, Virginia 22314 | 2 |
| 2. | Library, Code 0142<br>Naval Postgraduate School<br>Monterey, California 93940 | 2 |
| 3. | Department Chairman, Code 69<br>Department of Mechanical Engineering<br>Naval Postgraduate School<br>Monterey, California 93940 | 1 |
| 4. | Associate Professor M. D. Kelleher, Code 69Kk<br>Department of Mechanical Engineering<br>Naval Postgraduate School<br>Monterey, California 93940 | 1 |
| 5. | Professor M. M. Yovanovich<br>Department of Mechanical Engineering<br>University of Waterloo<br>Waterloo, Ontario<br>Canada N2L3Gl | 1 |
| 6. | LCDR Roy L. Brennon<br>USS Jason (AR-8)<br>FPO San Francisco, California 96644 | 1 |

Thesis
B80346
c.1

191675

Brennon
Investigation of the use of liquid crystal thermography study flow over turbomachinery blades.